5

Recent Advances on Face Recognition Using Thermal Infrared Images

César San Martin[1,2], Roberto Carrillo[1], Pablo Meza[2],
Heydi Mendez-Vazquez[3], Yenisel Plasencia[3], Edel García-Reyes[3]
and Gabriel Hermosilla[4]
[1]*Information Processing Laboratory, DIE, University of La Frontera*
[2]*Center for Optics and Photonics, University of Concepción*
[3]*Advanced Technologies Application Center, CENATAV*
[4]*University of Chile*
[1,2,4]*Chile*
[3]*Cuba*

1. Introduction

Nowadays it is possible to find several works on face recognition, where principally the visible range spectra is used. In addition, many techniques are tested on different databases and it is possible to identify the best method to use in applications such as: surveillance, access control, human robots interaction, people searching, identification, among others. In practice, the performance of any face recognition system depends on conditions such as viewing angle of the face, lighting, sunglasses, occlusion of the face by other objects, low resolution of the images, different distance of the subject to the camera, focus of the scene, facial expressions, changes of the subject along the time, etc. This type of variations have been simulated in several works in order to estimate the limitations and advantages of the classification methods developed at the moment. One of the most important effects to consider is the kind of illumination that exists in the scene, difference in lighting condition produces variations in the recognition rate, decreasing the effectiveness of the methods. In this way, infrared technology is introduced in face recognition in order to eliminate the dependence of lighting conditions, achieving satisfactory results even when exist the complete absence of illumination. Bebis et al. (2006); Chen et al. (2003); Chen (2005); Dowdall (2005); Friedrich (2002); Heo et al. (2005); Li et al. (2007); Singh et al. (2008); Socolinsky and Selinger (2002); Socolinsky et al. (2001); Zou et al. (2005; 2007) Conventional visible cameras are composed of a lens and a focal plane array, a detectors matrix that collect the input information in the range 0.4-0.75 μm. These sensors can be composed by CCD or CMOS technology, and their function is to translate the incident light flux to an electrical signal and then it is digitalized using analog to digital conversion. The infrared camera is similar, but the lens and the sensor technology are changed, i.e., the focal plane array is composed of a matrix of infrared sensor or detector with response ranging from the near wave infrared (0.75-1.4 μm) to the long wave infrared (8-15 μm).

The development of infrared detectors has been evoked principally in the use of semiconductors or photodetectors Piotrowski and Rogalski (2004). In this type of detectors the radiation is absorbed by the material by means of the photon interaction with the electrons, presenting at the same time a good signal to noise ratio and a swift answer. In order to achieve it, the detectors require a cooling system, this is the main obstacle for a massive use of this type of systems, since it represents an increase of the weight, volume and system cost. In the last years another class of commercial arrays have appeared and are compound with thermic detectors, in which the incident radiation is absorbed, provoking changes on the physical properties of the material. In contrast to the photodetectors, the thermic detectors can operate at room temperature, they are cheap and easy-to-use, but present modest sensibility and lower answering velocity Liu et al. (2007).

The imaging system presents different undesired kinds of noise, being the principals temporal or electronic noise and the Spatial or Fixed-Pattern Noise (FPN) Mooney et al. (1989); Pron et al. (2000). Temporal noise is typically modeled by additive gaussian white noise, and by definition it varies with time. This type of noise is due to the photon noise and reset noise, and can be reduced using frame averaging. On the other hand, the FPN is due to the nonuniform response presented by the individual detectors and dark current non-uniformity, the principal characteristic is that not change in time and this kinds of noise can affect the final result of the classification. The FPN effect is stronger at longer wavelengths, such as in Infrared Focal-Plane Arrays (IRFPA), producing a severe mitigation on the quality and the effective resolution of the imaging device. Therefore, a nonuniformity correction (NUC) Perry and Dereniak (1993) is a mandatory task for properly using several imaging systems. The study associated of the NUC algorithms represents a broad area of work, in which we are supported by many developed articles.

This chapter presents the behavior of several state-of-art facial classification methods using the infrared spectra, considering temporal and fixed-pattern noise. The principal motivation is to introduce the recent advances in infrared face recognition field, and the use of different data sets built with at least two different infrared cameras. The performance of the recognition system is evaluated considering temporal and spatial noise, in real and simulated scenario, keeping in mind that a computer simulation allow the possibility of controlling the signal to noise ratio and then, obtain more representative results. An infrared scene, acquired from a IR camera,present only one level of noise, but it is possible to consider 20 degrees of maximum rotation of the face and different facial expression.

Two mechanism are used: full image and segmented image. The first one consist on using all pixels of the image, and then, build the classification. In a segmented image, the region corresponding to the face image is separated from the background and the process is introduced to design the classification rule, and then, the recognition process is performed. In some cases, from segmented images is possible to build a characteristic vector that represent the principal feature in order to perform the classification. The principal advantage of segmentation and feature representation corresponds to the reduction of the dimensionality and then, the computing time. In this chapter, we use full image in order to obtain more representative evaluations of the noise effect on recognition task.

The algorithms will be tested on a database with different frames for each subject considering vocalization and facial expressions, allowing to construct a symmetric database with and without noise. The results shown different behavior of different recognition techniques considering temporal or fixed noise pattern.

In this work, two IR face databases are used. The first one has been collected by Equinox Equinox (2009) and consists of images captured using multiple camera sensors: visible, long-wave infrared (LWIR), mid-wave infrared and short-wave infrared spectra. Moreover, they use a special visible-IR sensors capable of taking images with both visible CCD and LWIR microbolometer in $8-14\mu m$ spectral range. The database consists of $3,244$ face images from 90 individuals captured with left, right and frontal lighting, and neutral and varying facial expression. Also include an eyeglasses condition since eyeglasses block the thermal emission. Only LWIR imagery are used, with a resolution of $320x240$ pixels and 12 bits per pixel.The images contain a fixed-pattern noise from captured image and is removed using NUC scene-based-method.
The second database consists of images captured using the CEDIP JADE UC camera with an operating range in $8-14\mu m$ with microbolometer detector-based. The database consists of 612 images corresponding to 6 images per 102 persons. The images containing expression and vocalization faces, with $320x240$ pixels and 14 bits of resolutions. The images are captured and corrected using two-point radiometrically calibration by means black bodie radiator, located in the Center for Optics and Photonic CEFOP laboratory. This second database is noise free and this condition permit to simulate fixed and temporal noise allowing to gain more representative results.
We are interesting in to study both cases, the noise-behavior of correlation filters and LBP face recognition system, considering two scenarios: identification and verification. In the first case, the performance is evaluated using the correct classification (CC) percent, defined as the ability of the system to identify new pattern or signature. In a verification scenario typically it confirms if a subject is valid or not for a given data set, measured by the false acceptance rate (FAR) and a false rejection rate (FRR). CC, FAR, and FRR are obtained for the cases with/without fixed noise and temporal noise. In this work, the performance results are obtained with the top match approach.

2. Non-uniformity and FPN noise in IR-FPA sensors

In an IR-FPA system, the main noise source is the FPA temporal noise: the FPA NU noise and the readout noise due to the associated electronic Milton et al. (1985). The FPN corresponds to any spatial pattern that does not change in time. Then, the NU in IR-FPA is added to the readout signal forming a FPN that degrades the quality of acquired data. Visually, the FPN is a pixel-to-pixel variation when a uniform infrared radiator is captured by the IR sensors. Typically, each pixel on the IR-FPA can be modeled in the instant n using a first-order equation given by Perry and Dereniak (1993):

$$Y_{ij}(n) = A_{ij}(n)X_{ij}(n) + B_{ij}(n) + V_{ij}(n), \tag{1}$$

where $Y_{ij}(n)$ is the readout signal, $X_{ij}(n)$ is the photon flux collected by the ij sensor, $A_{ij}(n)$ and $B_{ij}(n)$ are the gain and offset of the detector respectively, and $V_{ij}(n)$ is the additive temporal noise, usually assumed to be white gaussian random process.
In order to solve this problem, several NU compensation techniques have been developed Amstrong et al. (1999); Averbuch et al. (2007); Hardie et al. (2000); Harris and Chiang (1999); Narendra (1981); Pezoa et al. (2006); Ratliff et al. (2002; 2005); Scribner et al. (1991; 1993); Torres and Hayat (2002); Torres et al. (2003); Zhou et al. (2005). They can be divided into

calibration techniques and scene-based correction methods. The first group requires two uniform references from blackbody radiator at different temperatures, and by solving the system of equations, the gain and offset are obtained. The NU compensation is performed using the following equation:

$$\hat{X}_{ij}(n) = \frac{Y_{ij}(n) - \hat{B}_{ij}}{\hat{A}_{ij}}, \tag{2}$$

where $\hat{A}_{ij}$ and $\hat{B}_{ij}$ are the estimates of the gain and offset, and $\hat{X}_{ij}(n)$ is the estimated IR input irradiance.

The scene-based methods estimate gain and offset but the performance is limited by the amount of spatio-temporal information and the diversity of temperature in the image sequence. The condition of constant movement of the camera, to wich these methods are subject, is the main constraint for the scene-based methods. In addition, the requirement of a large number of frame also plays an important roll in a correct estimation.

A well-known scene-based NUC method is the constant statistics method proposed in Harris and Chiang (1999). The principal assumption of this method is that the the first and second moment of the input irradiance are equal to all sensors of FPA. Applying the mean and variance to equation (1), and assuming that the mean and standard deviation of X_n are 0 and 1, respectively, we can obtain the gain and offset from:

$$\hat{A}_{ij} = \sigma_{Y_{ij}} - \sigma_{v_{ij}}, \tag{3}$$

$$\hat{B}_{ij} = \mu_{Y_{ij}}. \tag{4}$$

In order to obtain a solution with low error estimation, it is required a good estimation of the mean and variance (large number of frames). To avoid this condition we assume that the readout data have a uniform distribution in a known range $[Y^{\min}, Y^{\max}]$, in such case the mean and variance can be obtained respectively from:

$$\mu_{Y_{ij}} = \frac{Y_{ij}^{\max} + Y_{ij}^{\min}}{2} \quad \wedge \quad \sigma_{Y_{ij}} = \frac{Y_{ij}^{\max} - Y_{ij}^{\min}}{\sqrt{12}}, \tag{5}$$

and then, the correction is performed using equation (2) with the values obtained from (3) and (4).

Another NUC method can by applied when the NU in the IR-FPA is mainly produced by the spatial variation in the offset, i.e., the gain $A_{ij}(n)$ is assumed a know constant given by the camera manufacturer. In this case, a one-point calibration is required in order to perform the NUC. If the offset is assumed constant for a particular time period t_c, it can be estimated recursively as:

$$\hat{B}_{ij}(n) = n^{-1} Y_{ij}(n) + n^{-1}(n-1)\hat{B}_{ij}(n-1), \tag{6}$$

and the FPN can be reduced by $Y_{ij}(n) - \hat{B}_{ij}(n)$. Also, the drift in time of the parameters t_d is such that satisfies $t_d \gg t_c$. This means that for a time greater than t_d a new estimation of the offset is necessary in order to perform an adaptive and continuous NUC.

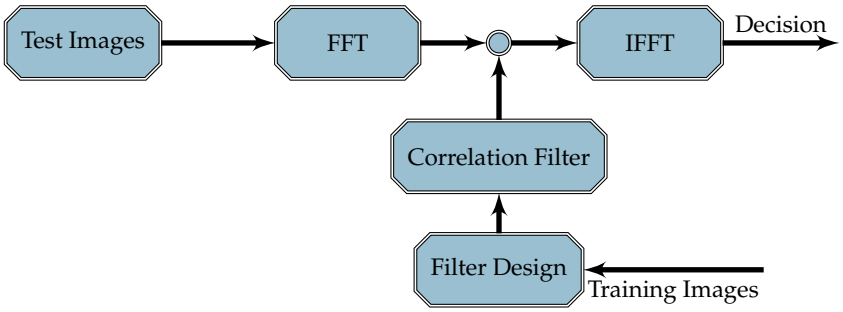

Fig. 1. The correlation process for face identification problems. Template correspond to the IR image set to design the correlation filters.

3. Face recognition methods

In this section, two traditional recognition methods are presented: correlation filters and local-binary pattern-based method. For both techniques a full image is used in order to build the classification rule. The aim of this is to evaluate the noise-tolerance of both methods when fixed and temporal noise are presented, degrading the quality of the acquired image in the input data.

3.1 Correlation filters

The correlation is a metric normally used to characterize the similarities between a reference pattern and a test pattern; this concept is widely use on recognition application, presenting a major degree of importance the use of the cross correlation obtaining the relative location of the object. Due to this analysis, the peak side lobe is consider as a classification metric. The cross correlation can by expressed as follow:

$$c(\tau_x, \tau_y) = \int\int T(f_x, f_y) R^*(f_x, f_y) e^{j2\pi(f_x\tau_x + f_y\tau_y)} df_x df_y \tag{7}$$

$$= IFT\{T(f_x, f_y) R^*(f_x, f_y)\}, \tag{8}$$

where $R(f_x, f_y)$ and $T(f_x, f_y)$ are the 2D fourier transform of the reference and test pattern respectively. The equation 7 can be interpreted as the test pattern being filtered through a filter with a frequency response $H(f_x, f_y) = R(f_x, f_y)$, generating the $c(\tau_x, \tau_y)$ (Fig. 1)
One of the many application of this concept correspond to the face recognition Kumar et al. (2004), allowing to perform the classification at the speed of light in an optical laser-based system, generating a peak of information for a successful recognition, fixing a threshold of approval for a negative result Kumar (1992).
The fourier transform in the correlation allows the use of displaced or clipped images because it has not have influence on the discernment of the classification system, which favors the image preprocessing. The peak response just indicates the level of displacement without directly affecting the magnitude.

3.2 Filter types

The correlation filter generation procedure depend on the images training set included in the database, which must be selected maintaining a format that is as representative as possible, depending on the image size, certain variations in facial expressions, the face position, etc. There are several types of filters, including: phase-only filter, minimum average correlation energy, noise-tolerant, and optimal tradeoff filter.

3.2.1 POF (Phase-Only Filter)

One advantage of this filter is because it only uses one image per subject for the filter generation, represented by the following expression Horner & Gianino (1984):

$$POF \ : \ h = \left(\frac{FT\{r(x,y)\}}{|FT\{r(x,y)|\}} \right)^{*}, \tag{9}$$

but is necessary to consider that h has a low sensitivity to potential changes on the test images.

3.2.2 MACE (Minimum Average Correlation Energy)

The MACE filter Casasent & Ravichandran (1992) is designed with the objective of minimizing the average energy in the correlation plane resulting from the training images, restricting the value at the origin with respect to a preset value. The solution is represented by:

$$MACE \ : \ h = D^{-1}X(X^{*}D^{-1}X)^{-1}u, \tag{10}$$

where u is a row vector containing the desired values for the correlation peak, X is the complex matrix where each column is a vectorized training image and matrix D is the diagonal matrix containing the spectral power of training images.

3.2.3 NTC (Noise-Tolerant Correlation)

Because the MACE filter generates a correlation peak more notorious, tends to amplify the high spatial frequencies and any input noise. It is for this reason that the NTC filter aims to minimize the sensitivity of the filter represented by:

$$NTC \ : \ h = C^{-1}X(X^{*}C^{-1}X)^{-1}u, \tag{11}$$

diagonal matrix C is defined as the spectral power density of noise.

3.2.4 TOF (Optimal Tradeoff Filter)

The TOF algorithm Réfrégier (1993) provides a compromise between the features of the MACE filter, which accentuates the peak for positive results and the NTC filter, which aims to reduce the variance of the output noise. In this case, it is necessary to assume the presence of white noise in order to approximate the matrix C as the identity matrix, with a factor α equal to 0.99. Each filter is defined as:

$$NTC \ : \ h = T^{-1}X(X^{*}T^{-1}X)^{-1}u \tag{12}$$

$$T = \alpha D + (1-\alpha)C. \tag{13}$$

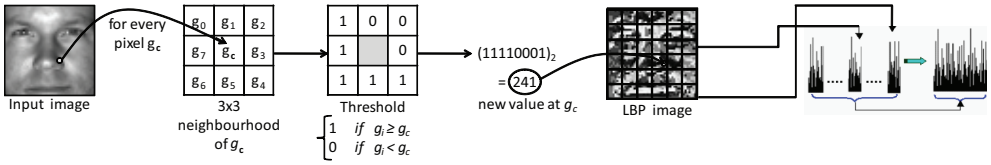

Fig. 2. Local Binary Patterns.

For analysis purposes, it will be use the TOF because of its robustness to evaluate the performance.

3.3 Local binary patterns

The use of the LBP operator in face recognition was introduced in Ahonen et al. (2004) and different extensions of the original operator have appeared afterwards Marcel et al. (2007). As it can be appreciated in Figure 2, the original LBP operator represents each pixel of an image by thresholding its 3x3- neighborhood with reference to the center pixel value, g_c, and considering the result as a binary number, called the LBP code. The image is then divided into rectangular regions and histograms of the LBP codes are calculated over each of them. Finally, the histograms of each region are concatenated into a single one that represents the face image. The Chi-square dissimilarity measure is used to compare the histograms of two different images.

3.4 Performance evaluation

In the diverse studies the analysis of the classification results depends on the characteristics of the system according to the structure that the database possesses; one of the most common is the peak-to-sidelobe ratio.

3.4.1 PSR (Peak-to-Sidelobe Ratio)

The correlation results can be compared by calculating the following Kumar & Hassebrook (1990):

$$PSR : p = \frac{peak - \mu}{\sigma}, \tag{14}$$

where the peak corresponds to the higher correlated output amplitude, the mean and standard deviation correspond to an outer area of fixed size around the peak resulting in the output image.

3.4.2 PCE (Peak-to-Correlation Energy)

A more accurate way of characterize the correlated output is through the calculation of Kumar & Hassebrook (1990):

$$PCE : p = \frac{|c(0,0)|^2}{\int_{-\infty}^{+\infty}\int_{-\infty}^{+\infty}|c(x,y)|^2 dxdy}, \tag{15}$$

which is defined as the ratio of the correlation peak $c(0,0)$ and the energy present in the correlation plane. The PCE value approaches infinity as c approaches a delta function. Thus, as desired, larger PCE values imply a sharper correlation peaks. However, the major reason for using the PCE over other available peak sharpness measures is its analytical convenience.

Since an identification measure only provides information if a classification is correct or incorrect, it is necessary to include some metric that allow to verify the performance of the classification itself. Typically face verification measures whether a subject is valid or not for a given set, that is why we define two sets of database, subjects valid and imposters, measured by the FAR and FRR.

3.4.3 FAR

The false acceptance rate points to the statistical calculation of those subjects classified correctly without belonging to the data base, represented by:

$$FAR = \left(\frac{\text{impostors accepted as valid subjects}}{\text{total number of invalid subjects}} \right). \tag{16}$$

3.4.4 FRR

The false rejection rate is a statistical complement of the previous measure, indicating the number of subjects rejected during the identification and belong to the database:

$$FRR = \left(\frac{\text{valid subjects rejected}}{\text{total number of valid subjects}} \right). \tag{17}$$

The FRR and FAR are directly affected by the threshold value defined in the identification. The variation of this value causes these rates vary inversely, being able to appreciate this effect in the distribution features seen in Fig. 3.

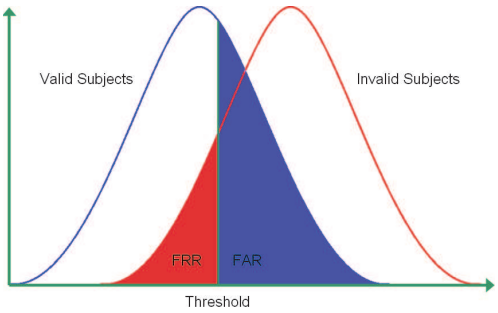

Fig. 3. Distribution of FAR and FRR for valid and invalid subjects.

For each threshold value, there is FAR and FRR defined as the identification, in an ideal case, the two curves should overlap at least as possible. Dependence between these two values can best be seen in Fig. 4, dependent on the statistical values calculated for value defined threshold, where the intersection on the curve indicates the critical threshold value to obtain an equal error rate (EER) for a $FRR = FAR$.

4. Face identification using Equinox infrared imagery

The Equinox Corporation database is composed of three 40 frame sequences from 90 persons, acquired in two days with three different light sources: frontal, left lateral and right lateral. The frame sequences were recorded while people were uttering vowels standing in a frontal pose, and three more images from each person were taken to capture the expression of,

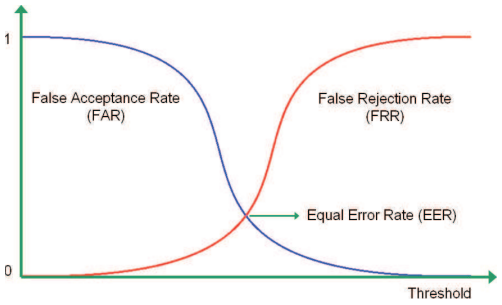

Fig. 4. EER as an intersection between FAR an FRR curves.

respectively to smile, frown and surprise. In addition, the complete process was repeated for those persons who wore glasses.
The LWIR images of Equinox are of 320x240 pixels size, they were represented as gray-scale images with 12 bits per pixels. The blackbody images are not available from Equinox (2009). Since much of the data is highly correlated, usually only a subset of the images is used for experimentation Heo et al. (2005); Socolinsky and Selinger (2002). In LWIR is not easy to precisely detect the facial features, so the images were not geometrically normalized and the different face images of one person are not aligned as can be appreciated in Figure 5. The size of the windows to divide the images for the LBP method was selected as 18x21 pixels taking into account this fact without decreasing the recognition performance.

4.1 FPN removal procedure

Considering the database Equinox (2009) it is possible to assume that the NU does not change in time. For instance, analyzing some images of two individuals (Fig. 5a and 5d) is possible to note that contain two typical distortions presents in IR imagery: dead-pixel and FPN. The first source of noise means that the detector always gives the same readout value independent of the input irradiance. The second is a FPN present in several sequences of individuals, but it is not possible to explain the nature of this FPN.
In order to remove the dead-pixel, it is possible to assume that the IR irradiance collected by the sensor ij is to be close to the neighbors around the sensor ij, and this value can be assumed the readout data. The FPN can be estimated using the equation (6) and then, reduced by perform the NUC process. Previously, the spatial offset of each image was removed resulting as shows Fig. 5b and 5e. The NUC images are shown in Fig. 5c and 5f, respectively. Note that the final images maintain the 320×240 resolution of the IR images of the database.

4.2 Data set for gallery and test

Following the procedure presented by Bebis et al. (2006); Socolinsky and Selinger (2002) we define multiple subsets using only three images of the vocal pronunciation frame sequence (vowel frames) and the three expression frames of each subject in each illumination condition:
VA: Vowel frames, all illuminations.
EA: Expression frames, all illuminations.
VF: Vowel frames, frontal illumination.
EF: Expression frames, frontal illumination.

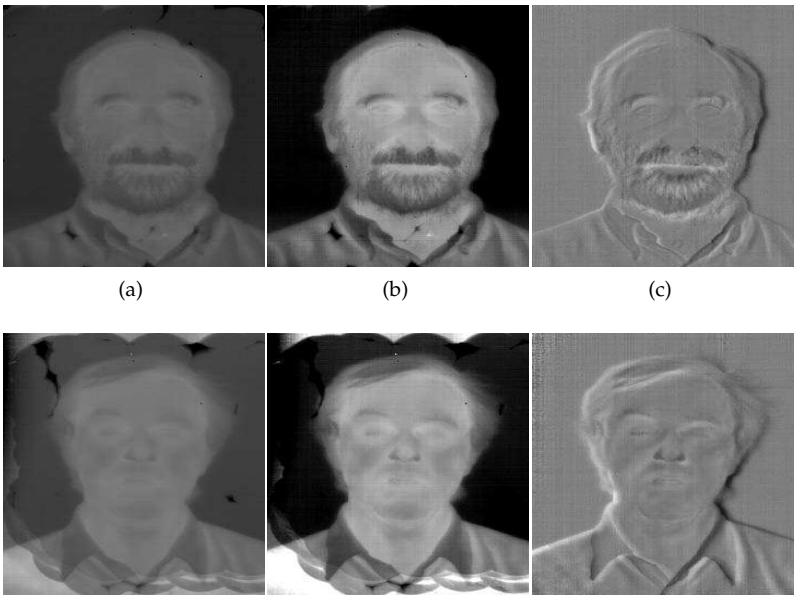

Fig. 5. Full size images of subject 2417 (a) and 2434 (d) from Equinox (2009) database. (b)(e) correspond to the spatial offset adjustment and (c) and (f) is with FPN removed. Its clear that the quality of the images are improved maintaining the 320x240 original spatial resolution.

VL: Vowel frames, lateral illuminations.
EL: Expression frames, lateral illuminations.
The performance of the correlation filter and LBP based matching are evaluated by using, each time, one set as gallery and another as a test set. Some of the subset combinations are not considered in the experiments since one subset is included in the other. Table 1 shows the performance of the evaluated methods.

4.3 Results using fixed-pattern-noise removal

From the first two rows of 1, corresponding to the use POF and TOF filter, is possible to appreciate the CC of 85.74% and 59.30% respectively, over the the original IR images. This implies that the performance of the POF filter in the original images is better than the TOF filter.
The LBP method on the other hand, presents an average of 97.3% of correct classification. Note that images are not geometrically normalized or cropped, and even a small localization error usually affects the appearance based methods. This performance is comparable with the best performance of an appearance based method obtained earlier with the same LWIR images by means of the Linear Discriminant Analysis (LDA) method Belhumeur et al. (1997), reported in Socolinsky and Selinger (2002) and summarized in Table 1. In this case, LDA achieves an average of 97.5% of correct classification. However, LBP has the advantage over the LDA method because it only needs one image per person in the gallery set, neither it requires a training set, which are very important properties of a face recognition system.

In order to improve the results and following the idea in San Martin et al. (2008), we applied the NU correction method discussed in section 2.2 prior to applying POF filter, TOF filter and the LBP representation, aiming to suppress the FPN present in the IR images. As can be appreciated in the second part of Table 1, the performance of POF and TOF filters with NUC in terms of CC are 97.93% and 99.60% respectively. Note that the performance of both filters is improved by using NUC method and the TOF filter CC is better than the one of POF filter. Surprisingly, with an average value of 93.3 percent, the performance with the NU correction using LBP was lower than without it. Inspecting the original and NU corrected images in Figure 5, it is apparent that although the NUC method suppresses fixed-pattern noise in the IR images, the random noise is magnified and the image texture is affected. Since LBP is a texture descriptor, it is sensitive to this kind of noise.
In order to support the hypothesis that the LBP method is sensitive to temporal random noise in LWIR images, we conducted the same experiments adding some random noise artificially to the original images. Table 5 displays the results of the experiments adding the random noise to the original LWIR images, with an average of 86.3 percent they confirm that LBP method decreases its performance in the presence of this kind of noise.

		without NUC						with NUC					
		VA	EA	VF	EF	VL	EL	VA	EA	VF	EF	VL	EL
POF filter	VA		84.64	83.77	84.39	82.40	84.14		98.13	99.13	98.50	98.50	98.88
	EA	84.08		85.58	89.33	87.08	89.33	97.94		97.94	98.13	97.94	97.75
	VF	89.76	81.90		84.27	80.77	84.27	100.00	98.25		98.75	97.50	99.25
	EF	97.19	80.52	91.39		85.58	91.76	99.44	96.44	97.75		96.07	97.94
	VL	83.52	85.27	82.77	84.52		83.77	99.75	98.50	98.88	98.75		99.00
	EL	81.27	90.07	84.46	86.70	87.64		95.13	96.44	95.51	95.69	95.88	
TOF filter	VA		54.56	55.31	54.81	53.43	55.68		100.00	99.75	100.00	99.88	99.88
	EA	52.25		56.74	67.79	64.42	60.30	99.63		99.63	100.00	99.81	99.81
	VF	60.05	48.69		52.18	51.31	55.93	100.00	100.00		100.00	100.00	100.00
	EF	88.20	53.18	73.22		60.49	78.65	99.81	99.81	99.44		99.25	100.00
	VL	52.93	55.81	54.68	54.81		53.93	99.88	100.00	99.75	100.00		99.88
	EL	51.12	60.30	67.60	54.68	76.04	98.13	98.13	98.31	98.88	97.75	98.88	
LBP	VA		98.13	97.75	98.50	99.25	95.13		88.89	95.63	87.89	95.38	90.14
	EA	97.67		93.77	98.44	97.67	100.00	97.67		94.94	93.77	98.05	97.67
	VF		98.13		97.00	97.38	95.51		85.77		92.51	90.26	86.02
	EF	99.24		99.62		99.24	95.08	98.48		98.86		98.48	94.70
	VL		98.13	96.63	96.63		96.63		91.26	93.63	83.65		90.76
	EL	97.74		92.83	95.09	98.49	96.60		93.96	93.21	98.11		
LDA	VA		99.60	98.30	96.20	99.60	99.30						
	EA	97.40		94.00	98.10	96.80	99.20						
	VF		100.00		97.00	98.80	98.60						
	EF	97.10		94.60		95.60	97.90						
	VL		99.50	97.40	95.80		99.60						
	EL	97.40		93.70	97.10	97.40							

Table 1. Correct classification percent with POF filter, TOF filter, LBP and LDA.

	VA	EA	VF	EF	VL	EL
VA		90.26	86.64	86.77	92.26	90.01
EA	87.03		81.06	80.16	87.55	91.05
VF		82.27		89.89	86.14	85.27
EF	89.14		88.76		85.61	83.33
VL		89.01	83.02	82.77		88.64
EL	86.79		80.50	82.64	87.92	

Table 2. Classification results with the LBP method adding random noise.

5. Face recognition performance using CEDIP JADE UC infrared imagery

The second database are collected using the CEDIP JADE infrared camera, with a focal plane array composed on type of detector capable of working without a cooling system known as microbolometer aSi and tuned at $8 - 14\mu m$. This data set consists of 6 images for 102 subjects considering vowel and expression variations, without illumination controls, generating the following codification:
V: Vowel frames.
E: Expression frames.
The infrared image are corrected using two-point calibration method, using the Mikron M345 black bodie radiatior. In this case, the goals is considering the following simulated scenarios:
- IR image without FPN and temporal noise.
- IR image with FPN with variance equal to 10, 20 and 30 percent.
- IR image with temporal noise with variance equal to 1, 5 and 10 percent.

In all cases, identification and verification problems are considered. In the first case, V (E) images are used as gallery and E (V) as test. In second experiment, the data set is divided in order to calculate the FAR, FRR and EER, and then, obtain the behavior of the classifications.

5.1 Identification results

In this experiment, a white noise is added in order to simulate the FPN and temporal noise. For all cases, five realization for each kind of noise and variance are considered, and the mean value is assumed as the mean correct classification using POF filter, TOF filter and LBP methods, respectively. In Table 3 the results considering FPN with 10, 20 and 30 percent are presented. In this case, the correlations filters strongly decrease their performance when the FPN noise variance increases. For the LBP method, the performance remains with low variability from the images without FPN noise. This mean that the LBP based method is robust to the FPN, not requiring a corrected infrared image.

5.2 Verification results

For this experiment, the database is divided into a training set composed of images of 34 subjects as clients, an evaluation set with images of the same subjects and a test set with 68 subjects. Three images per person are used for training, and the number of clients accesses is equal to $34x3 = 102$, i.e., the other three images of clients. The imposters accesses is given by the other 68 subjects of the database, and the number of accesses or comparisons can be summarized as:

		original image		FPN $\sigma = 10\%$		FPN $\sigma = 20\%$		FPN $\sigma = 30\%$	
		V	E	V	E	V	E	V	E
POF filter	V		91.50		91.50		91.44		91.57
	E	88.24		88.10		88.17		87.97	
TOF filter	V		98.69		84.12		81.18		76.47
	E	94.77		61.70		52.75		51.05	
LBP	V		99.35		97.32		97.19		97.52
	E	97.71		96.93		96.41		96.01	

Table 3. Correct classification percent with POF filter, TOF filter and LBP considering FPN.

		original image		noise $\sigma = 1\%$		noise $\sigma = 5\%$		noise $\sigma = 10\%$	
		V	E	V	E	V	E	V	E
POF filter	V		91.50		91.44		91.50		91.18
	E	88.24		88.24		88.24		88.17	
TOF filter	V		98.69		97.26		95.29		89.61
	E	94.77		94.44		92.81		88.17	
LBP	V		99.35		98.37		97.06		96.93
	E	97.71		96.86		96.80		95.23	

Table 4. Correct classification percent with POF filter, TOF filter and LBP considering temporal noise.

	Evaluation	Test
Clients accesses	$102(34x3)$	$204(68x3)$
Imposters accesses	$3366(102x33)$	$13668(204x67)$

Table 5. Distribution of the database to perform the verifications experiment.

		original image		FPN $\sigma = 10\%$		FPN $\sigma = 20\%$		FPN $\sigma = 30\%$	
		Evaluation	Test	Evaluation	Test	Evaluation	Test	Evaluation	Test
TOF	V	7.84	14.48	20.64	25.51	23.67	27.16	25.74	28.16
	E	11.76	14.72	34.63	43.00	34.62	43.01	38.29	44.45
LBP	V	3.92	5.42	7.45	7.15	7.50	7.74	8.48	8.41
	E	3.92	5.42	8.56	8.62	9.45	9.56	9.34	10.25

Table 6. Average Total Error Rate percent for the verifications experiment with TOF filter and LBP method considering FPN.

		original image		noise $\sigma = 1\%$		noise $\sigma = 5\%$		noise $\sigma = 10\%$	
		Evaluation	Test	Evaluation	Test	Evaluation	Test	Evaluation	Test
TOF	V	7.84	14.48	8.04	18.01	9.23	18.58	9.61	19.02
	E	11.76	14.72	12.54	15.41	12.44	15.46	16.09	20.60
LBP	V	3.92	5.42	3.92	5.10	6.00	6.77	9.34	10.51
	E	3.92	5.42	8.11	9.07	5.68	6.40	11.04	13.17

Table 7. Average Total Error Rate percent for the verifications experiment with TOF filter and LBP method considering temporal noise.

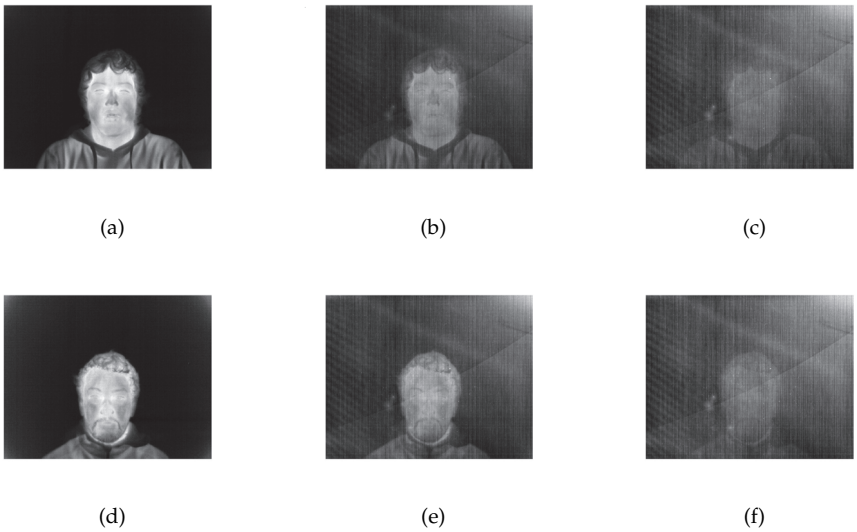

Fig. 6. Images of two different subjects from CEDIP JADE database: image without NUC (a)(d), with FPN 10% (b)(e) and FPN 30% (c)(f). The LBP method can be recognize the subject (c) and (f) with the same performance that the case (b) and (e).

The EER is the point at which the FRR is equal to the FAR in the evaluation set. The value obtained by the classification method at this point in the evaluation set is used as a threshold for the decision of acceptance or rejection in the test set. On the other hand, the Total Error Rate (TER) is the sum of FRR and FAR. The TER is used to evaluate the performance of the verification systems on the database. The lower this value, the better the recognition performance.

6. Remarks

From the results obtained using two infrared databases is possible to confirm that the LBP method is more robust than correlation filter when FPN is present, keeping in mind that this type of noise is natural in IR images, but from the results exposed is possible to consider that LBP does not require to apply NUC methods. An example is presented in Fig.6 (a) and (b), where two subjects images, initially noise-free, are afflicted due to the intrinsic properties of the FPN, drifting its parameters over time, decreasing the image quality, showing its effect on (b) and (e), and then (c) and (f). In this case, the results presented in this chapter allow to recognize the subject in image 6 (c) and (f) with the same error that (b) and (e), respectively. These results empirically demonstrate the ability of LBP method in order to perform good recognition task in infrared image with aggressive FPN.

7. Conclusion

In this chapter, is presented a review of various face recognition algorithms applied to an infrared database in order to evaluate the performance of each one, related with the problems

associated by working on this range of the spectrum. In particular, the use of infrared technology allows to formulate a face recognition system invariant to the illumination. For this, the long-wave spectra located at $8 - 14\mu m$ correspond to the emitted energy contraries with the visible spectra, in which the sensor collected the reflected energy. But the long-wave infrared spectra generate an intrinsic and special kind of noise (called nonuniformity), the fixed-pattern-noise (FPN) that correspond to a fixed pattern superimposed to the infrared image. In order to solve this problem, several nonuniformity correction techniques has been proposed, been an active area in the last years. The FPN is a pattern that slowly change in time. In several study, this kind of noise can be considered fixed or constant for almost two hours, but is depending of the technology of the infrared sensors.

In pattern recognition fields, is not habitual to study the noise robustness of classification techniques. A little kind of study consider only temporal noise, i.e., a pattern noise that change frame to frame, typically modeled as white noise. Our group include optoelectronic group and pattern recognition group, and the principal contribution is to present an infrared sensor description and the behavior of face recognition techniques considering this kind of sensors. In this chapter, firstly is introduced the concepts of FPN noise, and the objective is to study the behavior of two classical face recognition techniques when the nonuniformity of infrared cameras is not reduced or compensated. Then, the variation on the performance of each technique with and without nonuniformity correction method is obtained using two infrared databases. For both face recognition techniques identification and verification are considered.

Two face recognition techniques are used: correlation filters and local-binary pattern (LBP) based method. The results show that the LBP algorithm is one of the most robust to fixed pattern noise due to the inherent features of the correlation filters, the presence of any persistent pattern noise in time diminish the performance of the classification. In other hand, the temporal noise does not affect on a comparable level with the FPN, but the LBP still shows outstanding results.

As a counterpart to the analysis obtained by the different realizations of noise, it is clear that nonuniformity corrections generate an improvement over the correlation filters discernment, achieving competitive results with the other algorithms presented. Considering the case when TOF filter is used in Table 6, the TER for IR face recognition is 25.74%, and when the FPN is removed from images, the TER is reduced to 7.84%. Under these conditions, the techniques of non-uniformity correction behave like a promising feature extraction technique, extracting features to effectively and efficiently differentiate a subject from another.

Future work considering to build another database with more images per subject and repeat the process considering two weeks between acquisitions. The objective is to evaluate the robustness of LBP when real FPN is presented in the camera considering the past of time. Also, more face recognition should be included in order to find more FPN robustness techniques to perform face identification.

8. Acknowledgments

This work was partially supported by Center for Optics and Photonics CEFOP, FB0824/2008, Fondecyt 11090034, Proyecto de Iniciación en Investigación 2009, CONICYT, Chile, and by Universidad de La Frontera DIUFRO N^0 DI08-15.

9. References

Ahonen, T.; Hadid, A., & Pietikäinen, M. (2004) Face recognition with local binary patterns. *Lecture Notes on Computer Science* LNCS 3021, 469-481.

Armstrong, E.; Hayat, M.; Hardie, R.; Torres, S.; & Yasuda, B. (1999), Nonuniformity correction for improved registration and high-resolution image reconstruction in IR imagery. *Proceeding of SPIE*, 3808, 150-161.

Averbuch, A.; Liron, G. & Bobrovsky, B. (2008), Scene based non-uniformity correction in thermal images using Kalman filter. *Image and Vision Computing*, 25, 833-851.

Bebis, G.; Gyaourova, A.; Singh, A.; & Pavlidis, I. (2006), Face recognition by fusing thermal infrared and visible imagery. *Image and Vision Computing*24, 7, 727-724.

Belhumeur, P.; Hespanha, J. & Kriegman, D. (1997) Eigenfaces vs. Fisherfaces: Recognition using class specific linear projection. *IEEE Trans. Pattern Anal. Machine Intell.*,19,7, 711Ű720.

Casasent, D.; & Ravichandran, G. (1992), Advanced distortion-invariant minimum average correlation energy (MACE) filters, *App. Opt.* 31, (8), 1109-1116.

Chen, X.; Flynn, P.; Bowyer, & K. (2003), PCA-based face recognition in infrared imagery: baseline and comparative studies. *IEEE International Workshop on Analysis and Modeling of Faces and Gestures, AMFG.* 127-134.

Chen X.; Flynn P. & Bowyer K. (2005). IR and visible light face recognition, *Computer Vision and Image Understanding*, Vol. 99, No. 3, 332-358, ISSN 1077-3142.

Dowdall J.; Pavlidis I. & Bebis G. (2003). Face Detection in the Near-IR Spectrum. *Image and Vision Computing*. Vol. 21, No. 7, 565-578, ISSN 0262-8856.

Equinox IR Database, (2009) http://www.equinoxsensors.com/products/HID.html.

Friedrich G. & Yeshurun Y. (2002).Seeing People in the Dark: Face Recognition in Infrared Images. *Proceedings of the Second International Workshop on Biologically Motivated Computer Vision*, pp. 348-359, Vol. 252, 2002.ISBN 3-540-00174-3.

Hardie, R.; Hayat, M.; Armstrong, E.; & Yasuda, B. (2000), Scene-based nonuniformity correction using video sequences and registration. *Applied Optic*, 39, 1241-1250.

Harris, J.; & Chiang, Y. (1999), Nonuniformity correction of infrared image sequences using constant statistics constraint, *IEEE Trans. on Image Processing*, 8, 1148-1151.

Heo, J.; Savvides, M.; & Kumar, V. (2005), Performance Evaluation of Face Recognition using visual and thermal imagery with advanced correlation filters, *Conference on Computer Vision and Pattern Recognition, IEEE Computer Society*, pp.9-14.

Horner, J. & Gianino, P. (1984), Phase-only matched filter, *Applied Optics*, 23, 812-816 .

Kong, S.; Heo, J.; Abidi, B.; Paik, J.; & and Abidi, M. (2005), Recente advances in visual and infrared face recognition - a review. *Computer Vision and Image Undertanding*, 97, 1, 103-135.

Kumar, B. (1992), Tutorial survey of composite filter designs for optical correlators. *Appl. Opt.*, 31, 4774-4801.

Kumar, B.; Savvides, M.; Xie, C.; Venkataramani, K.; Thornton, J.; & Abhijit Mahalanobis (2004), Biometric Verification with Correlation Filters, *Appl. Opt.*, 43, 2, 391-402.

Kumar, B.; & Hassebrook, L. (1990), Performance measures for correlation filters. *App. Opt.* 29, 20, 2997-3006.

Li, S.; Chu, R.; Liao, S. & Zhang, L. (2007), Illumination invariant face recognition using near-infrared images. *IEEE Trans. Pattern Anal. Mach. Intell.*, 29, 4, 627-639.

Liu, X.; Fang, H.; & Liu, L. (2007), Study in new structure uncooled a-Si microbolometer for infrared detection. *Microelectronics Journal*, 38, 735-739.

Marcel, S.; Rodriguez, Y., & Heusch, G. (2007), On the Recent Use of Local Binary Patterns for Face Authentication. *International Journal on Image and Video Processing Special Issue on Facial Image Processing*.

Milton, A.; Barone, F.; & Kruer, M. (1985), Influence of nonuniformity on infrared focal plane array performance. *Opctical Engineering*, 24, 855-862.

Mooney, J.; Shepherd, F.; Ewing, W.; Murguia, J.; & Silverman, J. (1989), Responsivity nonuniformity limited performance of infrared staring cameras. *Optical Engineering*, 28, 1151-1161.

Narendra P. & Foss N. (1981). Shutterless fixed pattern noise correction for infrared imaging arrays. *Proceeding of SPIE*, pp. 44-51, Vol. 282, Washington, DC, USA, April 1981.

Perry, D.; & Dereniak, E. (1993), Linear theory of nonuniformity correction in infrared staring sensors. *Optical Engineering*, 32, 1854-1859.

Pezoa, J.; Hayat M.; Torres, S. & Rahman, M. (2006), Multimodel kalman filtering for adaptive nonuniformity correction in infrared sensors, *The JOSA-A Opt. Soc. of America*, 23, 1282-1291.

Piotrowski, J.; & Rogalski, A. (2004), Uncooled long wavelength infrared photon detectors. *Infrared Physics and Technology*, 46, 151-131.

Pron, H.; Menanteau, W.; Bissieux, C.; Beaudoin, J. (2000), Characterization of a focal plane array (FPA) infrared camera. *Quantitativa Infrared Thermography QIRT Open Archives, QIRT 2000*, http://qirt.gel.ulaval.ca.

Ratliff, B.; Hayat, M.; & Hardie, R. (2002), An algebraic algorithm for nonuniformity correction in focal-plane arrays. *The JOSA-A Opt. Soc. of America*, 19, 1737-1747.

Ratliff, B.; Hayat, M.; & Tyo, J. (2005), Generalized algebraic scene-based nonuniformity correction algorihtm. *The JOSA-A Opt. Soc. of America*, 22, 239-249.

Réfrégier, R. (1993). Optimal trade-off filter for noise robustness, sharpness of the correlation peaks, and Horner efficiency. *Opt. Lett.*, 32, 1933-1935.

San Martin, C.; Meza, P.; Torres, S. & Carrillo, R. (2008), Improved Infrared Face Identification Performance Using Nonuniformity Correction Techniques. *Lecture Notes on Computer Science*, LNCS 5259, 1115-1123.

Scribner, D.; Sarkady, K.; & Kruer, M. (1991), Adaptive nonuniformity correction for infrared focal plane arrays using neural networks.*Proceeding of SPIE*, 1541, 100-109.

Scribner, D.; Sarkady, K.; & Kruer, M.; (1993), Adaptive retina-like preprocessing for imaging detector arrays. *Proceeding of the IEEE International Conference on Neural Networks*, 3, 1955-1960.

Singh, R.; Vatsa, M. & Noore, A. (2008), Integrated multilevel image fusion and match score fusion of visible and infrared face images for robust face recognition. *Pattern Recogn.* 41, 3, 880-893.

Socolinsky, D. & Selinger, A. (2002), A Comparative Analysis of Face Recognition Performance with Visible and Thermal Infrared Imagery. In Icpr'02: *Proceedings of the 16Th International Conference on Pattern Recognition*, 4, 4.

Socolinsky, D.; Wolff, L.; Neuheisel, J.; & Eveland, C. (2001) Illimination invariant face recognition using thermal infrared imagery. *Proc. IEEE CS Conf. Comp. Vision and Pattern recognition*, 1, 527-534.

Torres, S. & Hayat, M. (2002), Kalman filtering for adaptive nonuniformity correction in infrared focal plane arrays. *The JOSA-A Opt. Soc. of America*, 20, 470-480.

Torres, S.; Pezoa, J. & Hayat, M. (2003), Scene-based nonuniformity correction for focal plane arrays using the method of the inverse covariance form, *Applied Optics*, 42, 5872-5881.

Zhou, H.; Lai, R.; Qian, S.; & Jiag, G. (2005), New improved non uniformity correction for infrared focal plane arrays. *Opctis Communications*, 245, 49-53.

Zou, X.; Kittler J. & Messer K. (2005), Face recognition using active near-ir illumination. *British Machine Vision Conference Proceedings*.

Zou, X.; Kittler J. & Messer K. (2007), Illumination Invariant Face Recognition: A Survey. In *First IEEE International Conference on Biometrics: Theory, Applications, and Systems*, 1-8.

Reviews, Refinements and New Ideas in Face Recognition
Edited by Dr. Peter Corcoran

ISBN 978-953-307-368-2
Hard cover, 328 pages
Publisher InTech
Published online 27, July, 2011
Published in print edition July, 2011

As a baby one of our earliest stimuli is that of human faces. We rapidly learn to identify, characterize and eventually distinguish those who are near and dear to us. We accept face recognition later as an everyday ability. We realize the complexity of the underlying problem only when we attempt to duplicate this skill in a computer vision system. This book is arranged around a number of clustered themes covering different aspects of face recognition. The first section on Statistical Face Models and Classifiers presents reviews and refinements of some well-known statistical models. The next section presents two articles exploring the use of Infrared imaging techniques and is followed by few articles devoted to refinements of classical methods. New approaches to improve the robustness of face analysis techniques are followed by two articles dealing with real-time challenges in video sequences. A final article explores human perceptual issues of face recognition.

How to reference
In order to correctly reference this scholarly work, feel free to copy and paste the following:

César San Martin, Roberto Carrillo, Pablo Meza, Heydi Mendez-Vazquez, Yenisel Plasencia, Edel Garcîa-Reyes and Gabriel Hermosilla (2011). Recent Advances on Face Recongition using Thermal Infrared Images, Reviews, Refinements and New Ideas in Face Recognition, Dr. Peter Corcoran (Ed.), ISBN: 978-953-307-368-2, InTech, Available from: http://www.intechopen.com/books/reviews-refinements-and-new-ideas-in-face-recognition/recent-advances-on-face-recongition-using-thermal-infrared-images

INTECH
open science | open minds

InTech Europe
University Campus STeP Ri
Slavka Krautzeka 83/A
51000 Rijeka, Croatia
Phone: +385 (51) 770 447
Fax: +385 (51) 686 166
www.intechopen.com

InTech China
Unit 405, Office Block, Hotel Equatorial Shanghai
No.65, Yan An Road (West), Shanghai, 200040, China
中国上海市延安西路65号上海国际贵都大饭店办公楼405单元
Phone: +86-21-62489820
Fax: +86-21-62489821